Available online at www.sciencedirect.com
SCIENCE DIRECT®
ELSEVIER
Quaternary Research 65 (2006) 324–335
QUATERNARY RESEARCH
www.elsevier.com/locate/yqres

Peak discharge of a Pleistocene lava-dam outburst flood in Grand Canyon, Arizona, USA

Cassandra R. Fenton [a,*], Robert H. Webb [b], Thure E. Cerling [c]

[a] GeoForschungsZentrum Potsdam, Telegrafenberg Haus B, D-14473 Potsdam, Germany
[b] U.S. Geological Survey, 520 N. Park Avenue, Tucson, AZ 85719, USA
[c] Department of Geology and Geophysics, 135 S. 1460 E., WBB 719, University of Utah, Salt Lake City, UT 84112, USA

Received 6 May 2005
Availble online 7 February 2006

Abstract

The failure of a lava dam 165,000 yr ago produced the largest known flood on the Colorado River in Grand Canyon. The Hyaloclastite Dam was up to 366 m high, and geochemical evidence linked this structure to outburst-flood deposits that occurred for 32 km downstream. Using the Hyaloclastite outburst-flood deposits as paleostage indicators, we used dam-failure and unsteady flow modeling to estimate a peak discharge and flow hydrograph. Failure of the Hyaloclastite Dam released a maximum 11×10^9 m^3 of water in 31 h. Peak discharges, estimated from uncertainty in channel geometry, dam height, and hydraulic characteristics, ranged from 2.3 to 5.3×10^5 m^3 s^{-1} for the Hyaloclastite outburst flood. This discharge is an order of magnitude greater than the largest known discharge on the Colorado River (1.4×10^4 m^3 s^{-1}) and the largest peak discharge resulting from failure of a constructed dam in the USA (6.5×10^4 m^3 s^{-1}). Moreover, the Hyaloclastite outburst flood is the oldest documented Quaternary flood and one of the largest to have occurred in the continental USA. The peak discharge for this flood ranks in the top 30 floods (>10^5 m^3 s^{-1}) known worldwide and in the top ten largest floods in North America.

Keywords: Grand Canyon; Colorado river; Pleistocene floods; Lava dams; Hydraulic modeling; Paleoflood indicators; Dam failure; Catastrophic floods

Introduction

Basalt flows from the Uinkaret volcanic field (Fig. 1) repeatedly dammed the Colorado River in western Grand Canyon between 100 and 630 ka (McIntosh et al., 2002; Fenton et al., 2004). During this time, at least 13 lava dams formed (Hamblin, 1994a), mostly in a 15-km reach of the canyon between Toroweap Valley (RM 179) and Whitmore Canyon (RM 188) (Fig. 2; distances along the Colorado River are conventionally referred to in river miles (RM) and are relative to RM 0 at Lee's Ferry, Arizona). The lava dams between RM 179 and RM 188 were 60 to 600 m high and impounded reservoirs that extended up to 518 km upstream (Hamblin, 1994a). The amount of time required to fill these reservoirs, based on current flow rates in the Colorado River averaging 18.5×10^9 m^3 yr^{-1} (Garrett and Gellenbeck, 1989), ranged from 2 days to 23 yr (Hamblin, 1994a).

Hamblin (1994a) speculated that lava dams in western Grand Canyon were stable and long-lived, further hypothesizing that each lake filled in with fine-grained sediments in no more than 3000 yr, eventually allowing the river to cascade over the face of each dam. Using Niagara Falls as an analogy, he suggested that waterfall-induced headward erosion gradually removed each dam over a period as long as 40,000 yr, but Hamblin (1994a) also states that most dams likely were removed within 20,000 yr. Likewise, Lucchitta et al. (2000) discuss erosion of western Grand Canyon lava dam and they link it to rapid aggradation of the river and major accumulation of basalt-rich gravels 48 km downstream of the lava dams between RM 207–209. Though they mention that these gravels represent extremely vigorous erosion of a dam, they still conclude that removal of the dam was a result of overtopping, headward erosion, and plunge-pool action. Both "gradual-removal" conceptual models assume that gravels were produced during

* Corresponding author.
E-mail address: crfenton@gfz-potsdam.de (C.R. Fenton).

0033-5894/$ - see front matter © 2005 University of Washington. All rights reserved.
doi:10.1016/j.yqres.2005.09.006

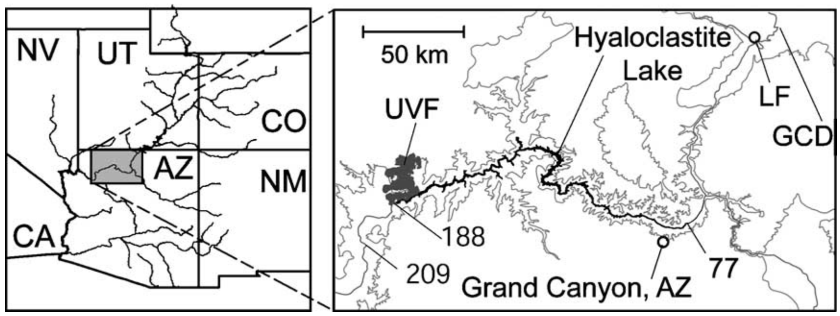

Figure 1. Map of the Colorado River through Grand Canyon showing the extent of Hyaloclastite Lake, a reservoir created by the Hyaloclastite Dam at RM 188.5 that reached upstream to RM 77. The contour line represents 1500 m elevation; the water-surface elevation of the lake was a maximum of 788 m. UVF = Uinkaret volcanic field; GCD = Glen Canyon Dam. 77, 188, and 209 refer to locations in river miles along the Colorado River.

the headward-erosion process and that these gravels were transported downstream and deposited in their present locations during typical river flows (Hamblin, 1994a; Lucchitta et al., 2000).

Because no evidence of lacustrine deposition remains within the confines of the former reservoirs (Kaufmann et al., 2002), there is no evidence that the lava dams produced long-lived lakes that eventually removed dams through gradual headward erosion. Furthermore, the abutments of lava dams were porous talus accumulations and unconsolidated river sediments (Fig. 3). Likewise, interaction of lava and water during dam formation created hydrothermal brecciation and fracturing. In combination, these conditions would have created inherently unstable dam footings (Fenton et al., 2002).

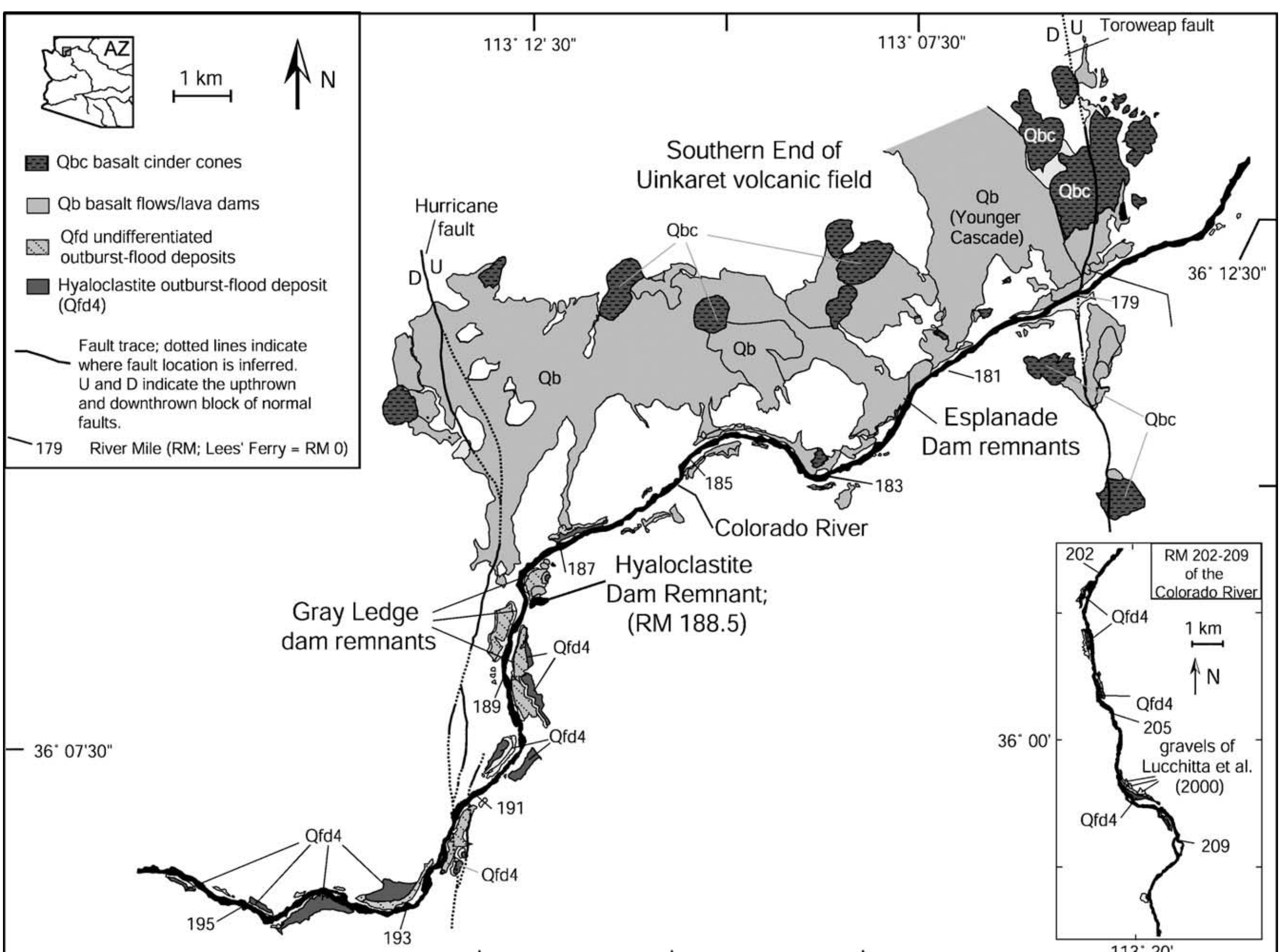

Figure 2. Map of the southern portion of the Uinkaret volcanic field showing the locations of Quaternary lava flows, lava dams, and Hyaloclastite outburst-flood deposits (modified from Fenton et al., 2004).

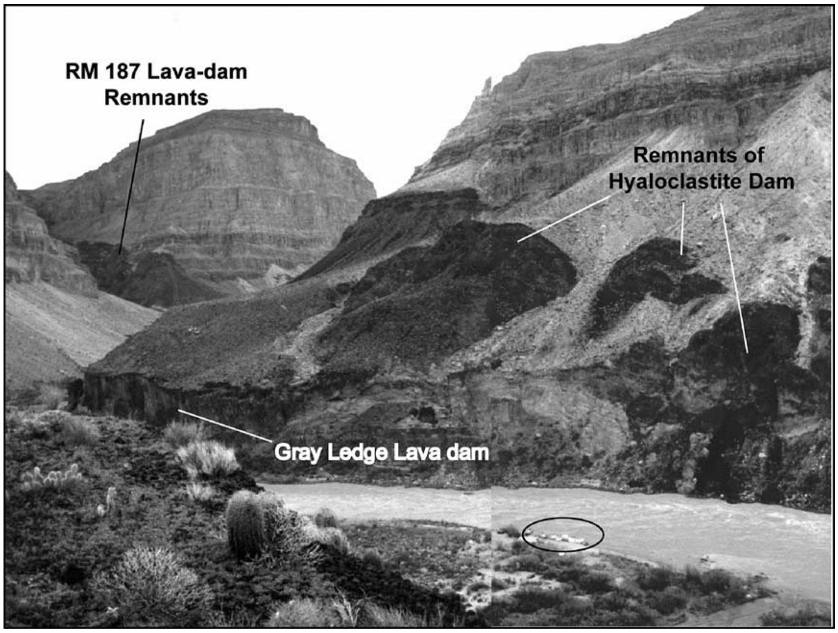

Figure 3. Upstream view of the remnants of the Hyaloclastite Dam across from Whitmore Rapids (RM 188.5) from the top of the Whitmore Cascade, an 180,000 yr lava flow (Fenton et al., 2004). Boats and tents on the beach (circled) provide scale. Note lava-dam remnants at RM 187 and a Qfd5 outburst-flood deposit (100,000 yr; Fenton et al., 2004) just upstream that overlies a remnant of the Gray Ledge Lava dam (100,000 to 190,000 yr; see text for details).

The flood-deposit evidence present downstream of the lava dams indicates that the headward-erosion hypotheses (Hamblin, 1994a; Lucchitta et al., 2000) are untenable for at least some of the lava dams.

Fenton et al. (2002, 2004) provided evidence of an alternative scenario in which some Grand Canyon lava dams breached catastrophically and, before overtopping, produced large outburst floods downstream. Five floods that occurred between 100,000 and 525,000 yr ago have been documented and geochemical correlations with upstream lava dams have been suggested (units Qfd1 to Qfd5 in Fenton et al., 2004). This scenario of catastrophic failure is more consistent with sedimentological, geochemical, and geochronological evidence preserved in the gravels between RM 187 and 222 (Fenton et al., 2002, 2004). In this paper, we report the results of hydrologic modeling of the flood wave representing one of these outburst floods, an event that occurred 165,000 yr ago with the failure of the Hyaloclastite Dam.

Description of outburst-flood deposits

The Hyaloclastite outburst-flood deposits are preserved between RM 189 and 209 (Fig. 2); they are the Qfd4 outburst-flood unit of Fenton et al. (2004). Using cosmogenic ^{3}He, the Hyaloclastite outburst-flood unit has been dated at 165,000 ± 18,000 yr (Fenton et al., 2004). This deposit is the most extensive, well preserved, and geochemically correlated of outburst-flood deposits in western Grand Canyon. It also has the least equivocal origin of the outburst-flood deposits: the Hyaloclastite Dam and associated outburst-flood deposit comprise tholeiitic basalt and have been geochemically correlated, whereas all other lava flows and lava-dam outburst-flood deposits in the area are composed of alkali-olivine basalts (Fenton et al., 2004).

The Hyaloclastite outburst-flood deposits are between 20 and 110 m thick, are greater than 82% basalt, and contain well-rounded to angular clasts ranging from hyaloclastite ash and lapilli to basalt boulders with a 5-m b-axis diameter. Fine-grained material in Hyaloclastite outburst-flood deposits is dominated by volcanic (basalt-glass) ash and lapilli (Fenton et al., 2002). These deposits decrease in elevation from 200 to 13 m above modern river level with distance downstream from the damsite (Fig. 4b). One deposit (RM 193.2) has large-scale foresets >40 m in height that indicate flow direction into the mouth of a side-canyon present at that location, which is the type of sedimentary structure one would expect where channel expansion and flow separation occur in an extremely large flood. Extremely large blocks (up to 8-m b-axis diameter) of local limestone bedrock in the deposits occur in positions where they could not have fallen from the surrounding cliffs, and we believe these blocks represent large-scale failure of dam abutments. The particle size of gravel deposits decreases from these blocks and boulders to cobbles with distance from the dam site. These features indicate deep, swift flood waters and a point source—specifically, a lava-dam failure—as the mechanism for deposition of the deposits.

We use the spatial distribution of outburst-flood deposits to define a water-surface profile from which the hydraulic characteristics of the flood can be estimated. The elevation of outburst-flood deposits decreases exponentially downstream, providing evidence of a water-surface profile for an unsteady flow (Fig. 4). This profile is typical of a flood wave that ensues during the rapid release of a reservoir at the onset of dam failure (Fread and Lewis, 1998). We interpret the flood deposits to be coarse-grained paleostage indicators of the type described by

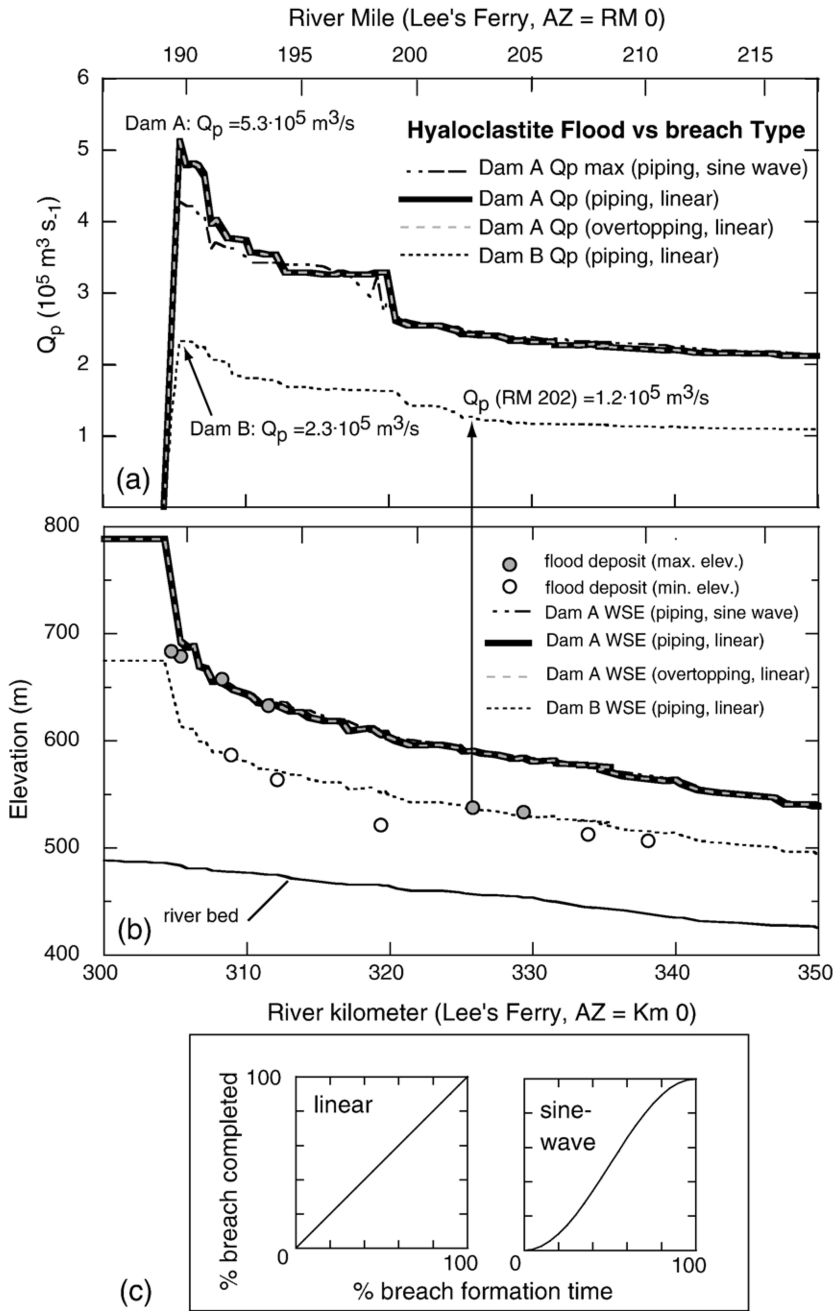

Figure 4. Q_p estimates (a) and associated water-surface elevations (WSE; (b)) of the Hyaloclastite outburst flood produced by the unsteady flood-wave model. Overtopping and piping as failure mechanisms produce identical results. Sine-wave breach formation (c) yields a significantly lower Q_p (b) but an indistinguishable change in water-surface elevation (a) from that of a linear breach formation (c). The arrow in panel b indicates the Q_p (a) associated with the flood deposit at this location and elevation.

Jarrett and England (2002), who found that deposits of this type are on average 15 mm higher than a known water surface. Unlike fine-grained slackwater deposits, the maximum height of which may be 0.50 to 0.90 m lower than the water surface (e.g., Erskine and Peacock, 2002; Webb et al., 2002), most Hyaloclastite outburst-flood deposits are representative of a maximum water-surface elevation. However, some deposits are degraded, eroded, or reworked and therefore represent only minimum high-water marks in our reconstructed water-surface profile (Fig. 4b).

Dam and channel geometry

Dam geometry

Although most of the Hyaloclastite Dam has been eroded, remnants of the original dam are preserved in a slump block at RM 188.5 (Fig. 3). A vertical exposure shows that the base of the dam overlies local limestone talus and is composed of 20 m of interfingered, brecciated lava flows, hyaloclastite ash and lapilli, and shattered pillow basalts (Fenton et al., 2004). Such basal features and talus would have provided fractures and conduits for piping of reservoir waters through the dam or its abutments. The presence of the talus beneath the abutments and the dam remnants in a slump block are consistent with the hypothesis that this dam was unstable. No absolute age exists for the Hyaloclastite Dam, but the dam is inset against and is younger than other lava flows in the immediate vicinity (180,000 to 315,000 yr; Fenton et al., 2004).

The geometries of the dam and its breach are not preserved owing to the extreme erosion associated with the failure and the antiquity of the remnants, so dam geometry is an independent variable in our analysis. The lava source (eruptive vent) was north of the canyon; almost all cinder cones in the Uinkaret volcanic field are on the north rim (Figs. 1 and 2). Remnants of the dam at RM 188.5 are up to 140 m above modern river level; however, these remnants have slumped and are not at their original position (Fig. 3). It is not possible to reconstruct the original height of these remnants, but we assume that they were no higher than 366 m above present-day river level based on the elevation of other dam remnants preserved at RM 187 on the north side of the river (Fig. 3). The RM 187 remnants have not been geochemically characterized, but they may be part of the Hyaloclastite Dam based on proximity to the slump-block. Hamblin (1994a) mapped the RM 187 remnants as part of his Esplanade lava-dam complex.

We assume that the Hyaloclastite Dam failed 'instantaneously,' or quickly enough such that there was negligible drawdown of the reservoir by the time the breach was fully developed. The primary evidence of 'instantaneous' failure is the presence and nature of flood deposits downstream (Fig. 4b; Fenton et al., 2004). This would result in critical flow created and controlled by the head of the maximum lake level (Walder and O'Connor, 1997). Peak discharge (Q_p) is related less to reservoir volume than to the depth and erosion rate of the breach because incomplete dam failure results in only partial draining of the lake (Walder and O'Connor, 1997). When breaching occurs, it is almost instantaneous in dams impounding reservoirs with a relatively large volume-to-depth ratio (Walder and O'Connor, 1997).

River channel geometry

Landform evidence in western Grand Canyon constrains channel geometry that existed 165,000 yr ago to near present-day conditions. This evidence includes: [1] the presence of Hyaloclastite outburst-flood deposits (RM 189.5) perched on a 320,000 ± 80,000 yr lava flow (Pederson et al., 2002) 180 m above present-day river level near the stratigraphically younger, inset Gray Ledge dam (Fig. 3), whose base and top are 14 and 45 m above river level, respectively; [2] the age of the lower of two basalt flows mapped as the Gray Ledge dam (Hamblin, 1994a), which is 193,000 ± 46,000 yr and is separated from the upper basalt flow (110,000 ± 30,000 yr) by a layer of well-sorted, imbricated basalt-rich river gravels (Fenton et al., 2004; McIntosh et al., 2002; Pederson et al., 2002); [3] the bases of Esplanade (K–Ar age: 210,000 ± 40,000 yr; Dalrymple and Hamblin, 1998), Younger Cascade (^3He_c age: 108,000 ± 11,000 yr, K–Ar age: 110,000 ± 53,000 yr; (Fenton et al., 2004; Dalrymple and Hamblin, 1998)), and Massive Diabase (K–Ar ages: 140,000 to 440,000 yr old (Hamblin, 1994a; Dalrymple and Hamblin, 1998; Wenrich et al., 1995)) lava-dam remnants that are presently exposed at, near, or below present-day river level; [4] the generally low production rate of debris flows from side-canyon tributaries in western Grand Canyon (Griffiths et al., 2004), which suggests relatively stable canyon walls (Hamblin, 1994b); and [5] the lowest exposure (17 m above present-day river level) available of a 110-m-thick Hyaloclastite outburst-flood deposit fills a paleochannel of the Colorado River at RM 194 (Fenton et al., 2004).

Considering this evidence in concert and noting the presence of the filled paleochannel at RM 194 with its base near present-day river level, it is likely that the Colorado River was no more than 17 m above of its modern vertical position at the time of the Hyaloclastite outburst flood. This uncertainty in river elevation is problematic in our hydraulic modeling, and we considered modeling the Hyaloclastite outburst flood with the channel bottom elevation 17 m above present-day level to provide a minimum-end range for the flood discharge. However, the largest uncertainty affecting accuracy of peak-discharge estimates is related to the dam-breach geometry, as demonstrated in our model results. Because we do not know the exact position of the canyon walls and channel bottom at that time, we use present-day canyon geometry (United States Geological Survey, 1924) as an approximation to route the flood wave resulting from the Hyaloclastite Dam failure.

The effects of regional tectonic activity on the longitudinal profile of the Colorado River cannot be ignored in reconstruction of channel geometry. The Hurricane fault crosses the Colorado River and has a measured vertical displacement in a Hyaloclastite outburst-flood deposit of 13 m near RM 191.5 (Fig. 1; Fenton et al., 2004). The normal fault has an average vertical displacement rate of 80 m/Ma (Fenton et al., 2001) and is downthrown to the west (Fig. 1). In our model, the maximum elevations of all Hyaloclastite outburst-flood deposits on the downthrown block downstream of RM 191.5 are increased by 13 m to correct for cumulative offset by the Hurricane fault for the past 165,000 yr.

Hydraulic reconstructions of unsteady discharge

Even during observed floods, many desirable geometric and hydraulic characteristics associated with peak discharges are unknown. The antiquity of the Hyaloclastite outburst-flood deposits creates considerable uncertainty in hydraulic parameters, and only a partial record of the flood can be obtained from the extant flood deposits. In our model, we chose to vary hydraulic parameters to model a water-surface profile that best matches the profile preserved in the Hyaloclastite outburst-flood deposits and to determine which variables had the greatest effect on our reconstructed water-surface profile and Q_p. The evidence for the dam position and the distribution of correlated Hyaloclastite outburst-flood deposits provides a basis for modeling of the dam breach and resulting flood. Only

Table 1
Variables, initial, and boundary conditions used in unsteady flow analyses (HEC-RAS) of Hyaloclastite outburst-flood scenario

HEC-RAS dam-breach variables[a]	Hyaloclastite outburst-flood scenario		
	Dam A[b]	Dam B[b]	
Dam height (m)/Elevation (m)	302/788	189/675	
Maximum dam width (m)	1598	716	
Minimum dam width (m)	90	90	
Dam bottom elevation (m)	486	486	
Dam length (upstream; m)	805	805	
Elevation of initial piping (m)	500	500	
Final breach bottom elevation (m)	486	486	
Reservoir volume released (m^3)	11×10^9	5×10^9	
Reservoir-release time (h)	31	27	
RM	River (km)	Q_p ($m^3\ s^{-1}$)	Q_p ($m^3\ s^{-1}$)
188.5	302.4	5.3×10^5	2.3×10^5
204.6	329.4	2.3×10^5	1.2×10^5
217.3	350.4	2.1×10^5	1.1×10^5

[a] In both scenarios, the model run time in both scenarios was 35 hr, a weir coefficient of 1.44 was used, and expansion and contraction coefficients were 0.3 and 0.1, respectively. The piping coefficient was varied from minimum and maximum allowable values of 0.6 to 0.8. The lowest, numerically stable value was 0.69 and it represents friction losses in piping conduits. A value of 0.8 represents a conduit with smooth walls (Brunner, 2002).

[b] 'Dam A' and 'Dam B' indicate scenarios that produced maximum and minimum peak discharge estimates for the Hyaloclastite Dam flood that produced associated water-surface profiles that matched elevations of preserved Hyaloclastite outburst-flood deposits. See text for details.

elevations of Hyaloclastite outburst-flood deposits that did not appear degraded or eroded were used as high-water marks in our model (Fig. 4).

Dam-breach geometry, lake volume, and model assumptions

In this study, we used a one-dimensional flow model (HEC-RAS 3.1.1; Brunner, 2002) to reconstruct and estimate the peak discharge (Q_p) of the Hyaloclastite outburst flood in western Grand Canyon. The dam-breach and unsteady-flow options in HEC-RAS 3.1.1 were used to simulate failure of the Hyaloclastite Dam.

A total of 103 channel cross-sections were used to simulate canyon geometry for flood routing in our model. They were extracted from 10-m digital-elevation models with an average spacing of 190 m along the channel. Cross-sections were generated for the dam site, at all Hyaloclastite outburst-flood deposits, and at hydraulic controls or expansions where significant off-channel storage of floodwaters could have occurred. Interpolated cross-sections were more tightly spaced just upstream and downstream of the dam to best numerically characterize the peak of the flood wave. We used a hydrograph for the upstream boundary condition and normal depth with a friction slope of 0.00131 as the downstream condition (Table 1). We chose a realistic, conservative 227 $m^3\ s^{-1}$ constant inflow to the reservoir because we wanted the model output to reflect dam-failure discharges and not be augmented by a larger discharge (i.e., flood stage during Pleistocene glacial conditions). This inflow value is realistic because it is less than the average annual discharge of 526 $m^3\ s^{-1}$ for the Colorado River over the past 450 yr (Stockton and Jacoby, 1976), which includes annual peak flows, and pre-Glen Canyon dam discharges from 1922 to 1963 range from 54 to 767 $m^3\ s^{-1}$ (U.S. Geological Survey National Water Information System; http://water.usgs.gov/nwis). Our selected inflow value was also the lowest constant discharge we could use in the model without it becoming unstable. The friction slope was estimated by calculating an average slope of the USGS-surveyed (1924) water-surface profile between RM 180 and 225. A friction slope could not be estimated by high-water indicators demarcated by Hyaloclastite outburst-flood deposits because the flood that emplaced them was an unsteady flood wave.

Large-volume reservoirs are needed for large-magnitude outburst floods. The Hyaloclastite Dam was up to 366 m high near RM 188.5 and impounded the Colorado River, creating the Hyaloclastite Lake that extended up to 179 km upstream (Fig. 1). Because lake volume controls, in part, how much water is released upon dam failure, we used a variety of dam heights and associated volumes in our model to represent various levels of the Hyaloclastite Lake and to gauge what volume was needed to reproduce the flood that emplaced the Hyaloclastite outburst-flood flood deposits. We only report results from two reservoir volumes—5×10^9 m^3 and 11×10^9 m^3—which we called Reservoirs A and B, respectively.

Reservoirs A and B had water-surface elevations of 788 and 675 m, and they would have been created by a Hyaloclastite Dam with heights of 302 and 189 m, respectively. Other dam heights within the 140–366 m height range were tested, and failures of these dams and release of their associated reservoir volumes did not reproduce water-surface elevations preserved in Hyaloclastite outburst-flood deposits. Dam heights of 189 and 302 m in our model produced associated floods with water-surface profiles that most closely matched and together bracketed the maximum elevations of Hyaloclastite outburst-flood deposits (Fig. 4a).

Reservoir A contained 11×10^9 m^3 of water and extended 179 km upstream to RM 77 (Fig. 1). Using the 450-yr average discharge of 16.6×10^9 $m^3\ yr^{-1}$ (Stockton and Jacoby, 1976), this reservoir would have filled in approximately 35 weeks with no leakage from the dam. Reservoir B would have held 5×10^9 m^3 of water and would have filled in 17 weeks without leakage. If the Hyaloclastite dam formed during periods of high runoff, (i.e., 8500 $m^3\ s^{-1}$) or low runoff (i.e., 227 $m^3\ s^{-1}$), Reservoir A would have filled between 2 weeks and 1.5 yr with no leakage. For comparison, Lake Powell, the reservoir behind present-day Glen Canyon Dam, has a maximum volume of 30×10^9 m^3 and initially filled in 17 yr in response to net inflows averaging 8.5×10^9 $m^3\ yr^{-1}$; the dam (RM −15) has a height of 178 m and is 25 km upstream from Lee's Ferry (Fig. 1). The actual fill time of Hyaloclastite Lake is unknown because historical flow volumes may not represent conditions when the dam formed. If the river had higher flow associated with glacial melting and runoff from its headwaters, the reservoir would have filled more rapidly.

Shape (particularly depth) and erosion rate of the breach are primary factors controlling peak discharge at the point of

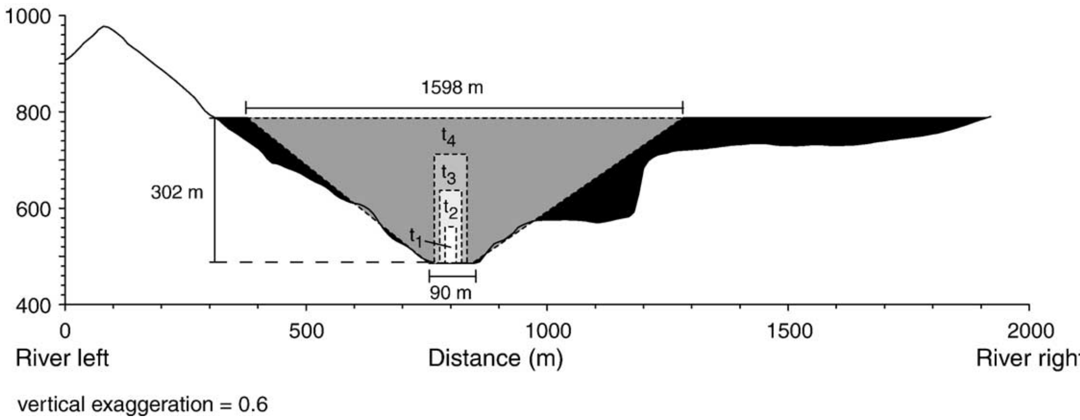

Figure 5. Cross-section of trapezoidal breach in the Hyaloclastite Dam (Dam A) approximated in the model. The breach forms in a linear fashion (times t_1–t_4) and is fully developed at t_4 (=1 h).

dam failure (Walder and O'Connor, 1997). When a tall dam fails, a very large Q_p is generated because of the exponential dependence of discharge to breach depth (Hamblin, 1994b). For both Dams A and B, we assumed complete failure of a trapezoidal breach (Fig. 5) and complete reservoir drainage. Dam-breach cross-sections typically are trapezoidal in constructed dams observed after historical failures (Walder and O'Connor, 1997, and references therein). The hypothesized breach in Dam A was 302 m deep and 90 and 1600 m wide at the narrowest and widest points; Dam B had an hypothesized breach depth of 189 m and a breach width of 90 to 716 m.

We assumed that the breaches in dams A and B fully developed in a linear fashion within 1 h (Fig. 6). This is a reasonable estimate considering that Teton Dam, a 93-m-high constructed earthen dam, failed completely in 2.6 h with a breach depth of 67 m and a width of 81 m (Fread and Lewis, 1998; O'Connor et al., 2002). An increased breach time (up to 5 h; Fig. 7) in our model decreased both Q_p and the water-surface elevations near the breach in the Hyaloclastite Dam and just downstream but produced negligible differences in water-surface elevation near RM 202 (Fig. 6). The two mechanisms that could have created the breach—piping and overtopping—produced identical flood-wave discharges and water-surface profiles (Fig. 4).

We compared the results of a sine-wave breach formation with that of the linear-breach formation. Although Q_p for the sine-wave breach formation was 8.5×10^4 m^3 s^{-1} lower than Q_p for the linear breach, there was no noticeable difference in water-surface profiles produced by both breach-formation types (Fig. 4). The unsteady flow model is very susceptible to numerical instability when using a sine-wave breach, so the linear-breach formation was used in all other dam-failure scenarios.

Although the lava dam most likely had an asymmetrical geometry created by a lava flow entering a deep bedrock canyon, the model was numerically unstable when trying to simulate a dam with asymmetrical geometry. Presumably, the dam would have been higher in elevation on the canyon wall nearest the volcanic vent, where lava would pile up before moving upstream, downstream, and across the canyon.

In both dam-failure scenarios (A and B), Manning's n values ranged from 0.025 to 0.10, where the highest values were used nearest the breach (Fig. 7). Values were chosen from a table with associated n value descriptions (Brunner, 2002). Values of n near the downstream boundary condition (RM 275; not shown in Fig. 7) ranged from 0.025 and 0.035, where flow became essentially steady. Although Q_p varied by 12%, the resultant water-surface elevation at this location showed negligible variation (3%) with Manning n. Variation of the n values for a given scenario (i.e., failure of Dam A) did not change Q_p or water-surface elevations enough to produce one water-surface profile that matched elevations of Hyaloclastite outburst-flood deposits, indicating that a range of discharges, created by scenarios A and B, is required to encompass the maximum elevations of the Hyaloclastite outburst-flood deposits.

Higher n values produce a steeper exponential curve near the dam breach, and the higher roughness could reflect the high debris load from the dam failure as well as energy losses associated with free-surface deformation and waves. Variation of n values near the breach caused a 10-m difference in water-surface elevation, and a difference of 3.6×10^4 m^3 s^{-1} in Q_p (Fig. 7). Because we have no objective way to account for channel aggradation nearest the breach, our maximum Q_p may be overestimated; however, uncertainties in the geometries of the dam and its breach are the largest source of uncertainties in Q_p and the water-surface profile.

Results of hydraulic modeling

We estimated that a maximum Q_p ranged from 2.3×10^5 to 5.3×10^5 m^3 s^{-1} for the outburst flood produced at the breach in the Hyaloclastite Dam (RM 188.5) using associated breach geometry and reservoir volumes for Dams A and B. At 48 km downstream from the dam, the two Q_p attenuated to 1.1×10^5 and 2.1×10^5 m^3 s^{-1}, respectively (Fig. 4a; Table 1). Scenario A resulted in a Q_p that reproduced water-surface elevations of Hyaloclastite outburst-flood deposits closest to the lava dam but overestimated deposit heights downstream (Fig. 4). Because 40-m-high, cross-stratified foresets are present in downstream deposits (RM 193.2), it is possible that these deposits were

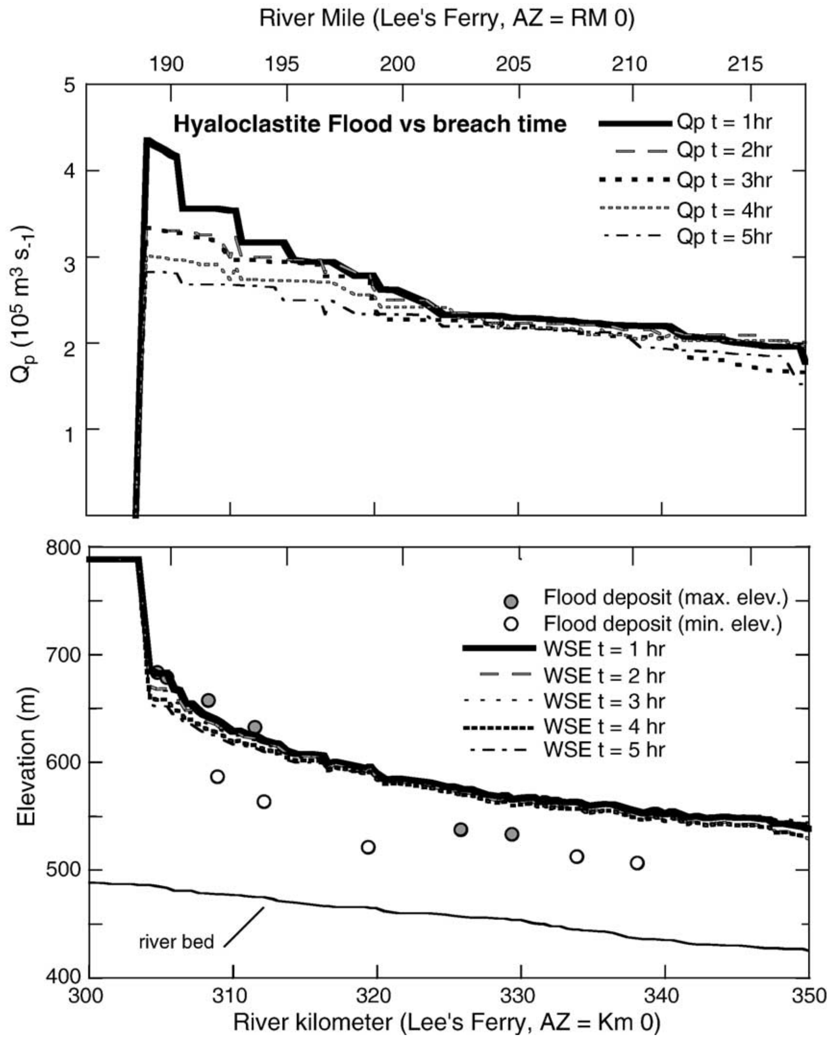

Figure 6. Changes in estimated Q_p and water-surface elevations (WSE) of the Hyaloclastite Dam outburst flood with varying breach-formation times.

submerged and may not represent the maximum stage of peak discharge. Dam failure and release of the smaller Reservoir B produced a Q_p of 2.3×10^5 m^3 s^{-1}, which is not large enough to reproduce the stage of Hyaloclastite outburst-flood deposits nearest the dam site; however, the flood wave did reproduce the stage of deposits 23 km downstream (Fig. 4b) with a Q_p of 1.2×10^5 m^3 s^{-1} at RM 202. Elevations of these deposits indicate that the flood wave was approaching steady flow. The maximum elevations preserved in flood deposits at RM 189.3 and 193.2 might be achieved by release Reservoir B if we assume that debris from the failed lava dam raised river level immediately downstream from the dam; however, we have no way of simulating this deposition, which likely was interacting with the flood wave. It is possible that our reconstructed peak discharges of 1.2×10^5 to 5.3×10^5 m^3 s^{-1} are underestimates, if in fact, the flood deposits required a larger water-column depth above their maximum elevations. Although deposition of fine-grained flood sediments rarely occurs at peak stages (Erskine and Peacock, 2002), coarse-grained particles indicative of more energetic flows typically are at or slightly higher than the average peak stage (Jarrett and England, 2002). However, there is no way to systematically quantify this for 165,000-yr-old deposits, given all of the uncertainties in the Pleistocene dam and reservoir geometries. We surmise that our Q_p estimates are reasonable and conservative based on the field evidence that is available for interpretation. We acknowledge the uncertainty in paleostage indicators by presenting a range in peak discharges for this outburst flood.

The results from scenarios A and B indicate that failure released 5×10^9 to 11×10^9 m^3 of water in 27 to 31 h (Table 1). There is no persistent evidence of the duration of this flood, but outburst floods typically are of short duration driven by the reservoir volume and mode of dam failure. The Teton Dam failure drained a reservoir holding 3×10^8 m^3 of water in less than 10 h (Fread and Lewis, 1998). Likewise, in August 2002, draining of Russell Lake, a modern lake formed by a glacial dam, released 3.13×10^{11} m^3 of water over 36 h, producing a Q_p of 1×10^5 m^3 s^{-1} (Trabant et al., 2003).

If the Hyaloclastite Dam failed through piping before overtopping could occur, the lifespan of the dam was less than 1.5 yr, the fill time under current flow volumes. The absence of non-volcanic fine-grained material (i.e., quartz-rich silts and sands) in Hyaloclastite outburst-flood deposits also attests to the short life-span of the Hyaloclastite Dam; the reservoir had

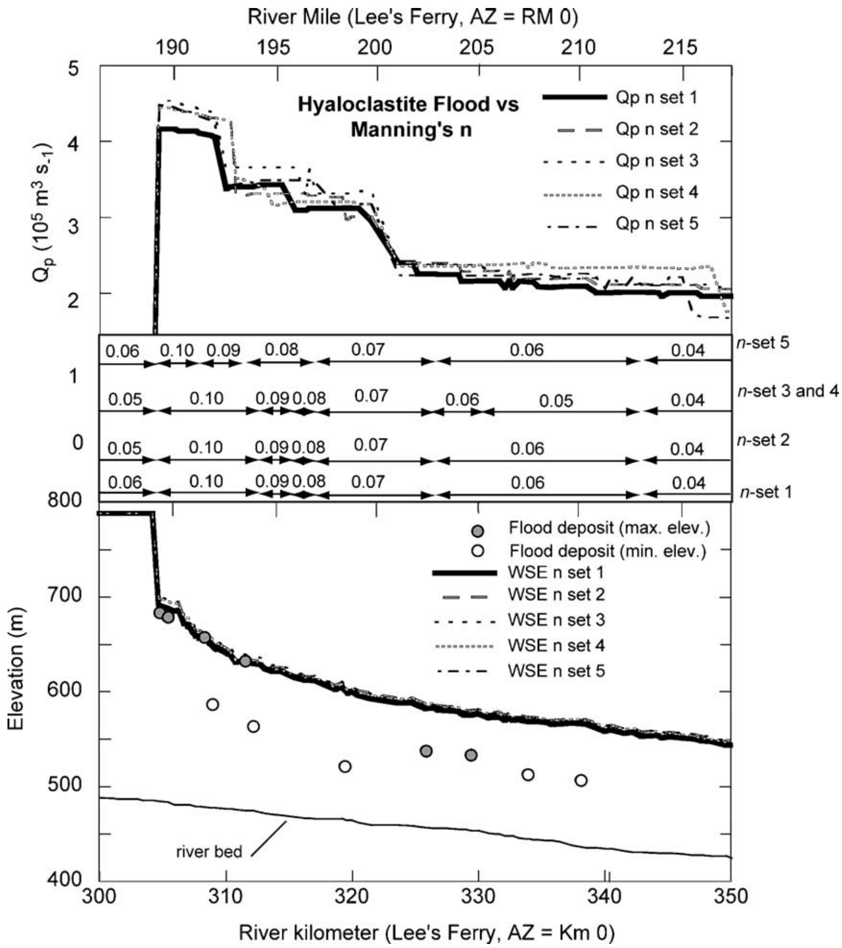

Figure 7. Changes in estimated Q_p and water-surface elevations (WSE) of the Hyaloclastite outburst flood with variation of Manning's n values (Dam A scenario). n values do not vary vertically or horizontally within a cross-section. The downstream boundary condition uses the following sets of Manning's n values: (set 1) 0.025; (set 2) 0.030; (set 3) 0.030; (set 4) 0.025); and (set 5) 0.030. Manning's n set 1 is used in Figure 4, our final best-fit Q_p and WSE estimates.

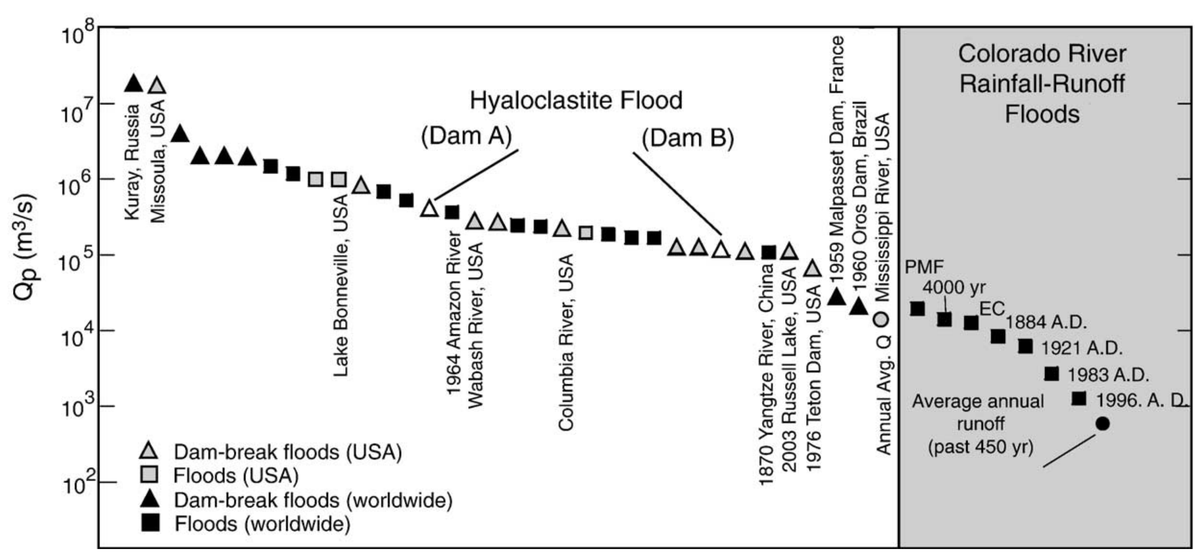

Figure 8. Graph showing the largest floods known worldwide, select large Colorado River floods, and peak-discharge estimates for the Hyaloclastite outburst flood (Table 2). White triangles labeled 'Dam A' and 'Dam B' represent the two Q_p estimates for the Hyaloclastite outburst flood. The dam-break floods refer to outburst floods resulting from the failure of natural and constructed dams. PMF = Probably Maximum Flood; EC = Envelope Curve; "4000 yr" refers to a prehistoric Colorado River flood (O'Connor et al., 1994).

Table 2
Comparison of maximum and minimum Hyaloclastite outburst-flood flood peak-discharge estimates to documented worldwide floods (>10^5 m^3 s^{-1}), constructed-dam-failure floods (>10^4 m^3 s^{-1}), and select Colorado River floods (at Lee's Ferry, AZ)

Flood/River	Mechanism	Peak discharge (10^6 m^3 s^{-1})
1. Kuray, Russia	Ice-dam failure	18
2. Missoula, USA	Ice-dam failure	17
3. Darkhat Lakes, Mongolia	Ice-dam failure	4
4. Jassater Lakes, Russia	Ice-dam failure	2
5. Yaloman Lakes, Russia	Ice-dam failure	2
6. Ulymon Lakes, Russia	Ice-dam failure	1.9
7. Katla, Iceland	Sub-glacial volcanic eruption	1.5
8. Lake Agassiz, Canada	Proglacial-lake overflow	1.2
9. Aniakchak, USA	Caldera-lake breach	1.0
10. Lake Bonneville, USA	Lake-basin overflow	1.0
11. Lake Regina, CanadaSA	Ice-dam failure	0.8
12. Jökulsá á Fjöllum, Iceland	Sub-glacial volcanic eruption	0.7
13. Indus River, Pakistan	Landslide-dam failure	0.54
14. Hyaloclastite outburst-flood flood (Dam A), Colorado River, USA	Lava-dam failure	0.53
15. Amazon River, Brazil	Rainfall	0.37
16. Wabash River, USA	Ice-dam failure	0.27
17. Toutle River, USA	Landslide-dam failure	0.26
18. Amazon River, Brazil	Rainfall	0.25
19. Amazon River, Brazil	Rainfall	0.24
20. Columbia River, USA	Landslide-dam failure	0.22
21. Lake Agassiz, CanadaSA	Proglacial-lake overflow	0.20
22. Lena River, Russia	Ice-jam and snowmelt	0.19
23. Lena River, Russia	Ice-jam and snowmelt	0.17
24. Lena River, Russia	Ice-jam and snowmelt	0.17
25. Lake Agassiz, USA	Ice-dam failure	0.13
26. Porcupine River, USA	Ice-dam failure	0.13
27. Hyaloclastite outburst-flood flood (Dam B), Colorado River, USA	Lava-dam failure	0.12
28. Russell Fjord, USA	Ice-dam failure	0.11
29. Yangtze River, China	Rainfall	0.11
30. Russell Lake (2003), USA	Ice-dam failure	0.10 [a]
31. Teton Dam (1976), USA	Constructed dam failure	0.065
32. Malpasset Dam (1959), France	Constructed dam failure	0.028
33. Oros (1960), Brazil	Constructed dam failure	0.020
34. Mississippi River (1993), USA	Rainfall	0.014 [b]
Select Colorado River Floods		
Probable maximum flood (PMF)	(Predicted) Rainfall	0.0197 [c]
Prehistoric flood (4 ka)	Rainfall	0.0142 [d]
Envelope curve (Enzel et al., 1993)	Rainfall	0.013 [e]
Colorado River (1884), USA	Rainfall	0.0085 [f]
Colorado River (1921), USA	Rainfall	0.0063 [f]
Colorado River (1983), USA	Rainfall	0.0028 [f]
Colorado River (1996), USA	Rainfall	0.0013 [f]
Average annual runoff (past 450 yr)	Rainfall	0.000527 [g]

Note. Table modified from O'Connor et al. (2002), where references for each of these floods are listed, notwithstanding the Hyaloclastite outburst-flood flood.
[a] Trabant et al. (2003).
[b] Average annual discharge into Gulf of Mexico 14,000 m^3 s^{-1} (Walker et al., 1994).
[c] Bureau of Reclamation, 1990.
[d] O'Connor et al. (1994).
[e] Enzel et al. (1993).
[f] Discharge data from U.S. Geological Survey National Water Information System (http://water.usgs.gov/nwis).
[g] Stockton and Jacoby (1976).

insufficient time to accumulate significant non-volcanic lacustrine sediments from upstream sources (Fenton et al., 2002).

Discussion and conclusions

Failure of the Hyaloclastite Dam, which formed 165,000 yr ago in western Grand Canyon from lava flows emanating from north of the canyon rim, created a high-magnitude outburst flood that left paleostage-indicator evidence over a 32-km reach. We used two scenarios of dam height, reservoir volume, and failure mechanisms to produce water-surface profiles of unsteady flow. The flood waves created by the failures of dams A and B, representing two different heights and associated reservoir volumes for the Hyaloclastite Dam, bracket the maximum elevations of Hyaloclastite outburst-flood outburst flood deposits and yield associated estimates of the peak discharge.

No single flood wave matched the water-surface profiles preserved in outburst-flood deposits. Variation in breach-formation type, breach-formation time, breach geometry, and Manning's n was used to bracket the uncertainty in peak discharge. Because of the antiquity of the Hyaloclastite outburst-flood deposit and changes in canyon and channel geometry during the intervening years, there is too much uncertainty in the extant flood evidence to provide an absolute peak discharge for this flood. Therefore, we conclude that our model constrains the magnitude of the outburst flood to 10^5 m^3 s^{-1}, with a maximum Q_p at the dam breach of 5×10^5 m^3 s^{-1}.

For most rivers, the peak discharge of a dam-break flood is usually much larger than rainfall-runoff or snowmelt floods (Fread and Lewis, 1998). The Hyaloclastite Dam outburst flood dwarfs all known Holocene and historic floods produced by meteorological conditions in the upper Colorado River basin (Fig. 7). The largest historic flood through Grand Canyon was between 5900 m^3 s^{-1} (Topping et al., 2003) and 8500 m^3 s^{-1} (http://water.usgs.gov/nwis) in 1884. One prehistoric flood that occurred 4 ka had a range in peak discharge of 13,600–14,200 m^3 s^{-1} (O'Connor et al., 1994). Enveloping curves suggest that the largest Holocene runoff flood would be approximately 13,000 m^3 s^{-1} (Enzel et al., 1993), and the probable maximum flood for the Colorado

River in Grand Canyon is calculated to be 19,700 m^3 s^{-1} (Bureau of Reclamation, 1990). Even our lowest Q_p of 1.2×10^5 m^3 s^{-1} (RM 202) is an order of magnitude larger than both the largest Holocene runoff flood and the probable maximum flood for the Colorado River (Fig. 8).

Despite its peak discharge, the Hyaloclastite Dam failure and subsequent outburst flood probably had little effect on incision of the Colorado River or overall development of the Grand Canyon. According to our hydraulic modeling, the flood lasted only about 30 h; the short duration of this flood would have exerted relatively minimal stream power to the bed, banks, and canyon walls compared to more sustained floods with lower discharges. Floods with large peak stream power, but of short duration and low total energy expenditure are ineffective agents of geomorphic change in alluvial or bedrock channels, because of their short duration (Costa and O'Connor, 1995). It is likely, however, that lava-dam outburst floods caused local bed scour as well as considerable aggradation of volcanic debris.

In addition, lower incision rates are reported (Lucchitta et al., 2000; Pederson et al., 2002) in western Grand Canyon relative to eastern Grand Canyon for the past 630,000 yr, the time during which lava dams periodically existed in the western canyon (100,000 to 630,000 yr ago). The difference in incision rates may reflect the ineffective erosive power of lava-dam outburst floods in western Grand Canyon, overloading of the river system with volcanic debris, or possibly Holocene alluvial fill masking depth to bedrock (Hanks and Webb, in press). Even with the substantiation of at least five lava-dam failures (out of 13 documented lava dams; Hamblin, 1994a), it is possible that some lava dams were persistent and stabilized the channel, stalling downcutting. The amount of time and energy expended removing lava-dam material may have been considerable, decreasing the potential for bedrock incision compared with other reaches upstream unaffected by lava dams.

Comparison to large floods known worldwide

Worldwide, the largest floods have been caused by the failure of ice dams (Baker and Nummedal, 1978; O'Connor, 1993; O'Connor et al., 2002 and references therein; Huscroft et al., 2004), whereas our study quantifies outburst-flood discharges related to failure of a lava dam. All known floods with discharges greater than 5×10^5 m^3 s^{-1} resulted from the rapid release of water stored behind natural dams or within glaciers, regardless of the size of their catchment area (Table 2; Fig. 8; O'Connor et al., 2002). The best-known examples of these are the Kuray Flood (1.8×10^7 m^3 s^{-1}) in Russia and the Missoula Flood (1.7×10^7 m^3 s^{-1}) in the Pacific Northwest (USA), which resulted from the failures of glacial-ice dams (O'Connor et al., 2002, Baker and Nummedal, 1978; Fig. 8).

Outburst floods also result from rapid melting of glaciers, failure of natural and constructed dams, lake overflows or breaches (Teller and Thorleifson, 1987; Walder and Driedger, 1994; Waythomas et al., 1996; O'Connor et al., 2002). For example, overflow of Lake Bonneville initiated a 1.0×10^6 m^3 s^{-1} flood on the Snake River in Idaho, USA. The 1976 failure of the Teton Dam in Idaho produced the largest flood (6.5×10^4 m^3 s^{-1}) resulting from the failure of a constructed dam (Fread and Lewis, 1998; O'Connor et al., 2002). The peak discharge of the Hyaloclastite Dam outburst flood is approximately double that resulting from the Teton Dam failure and possibly half that of the Lake Bonneville flood.

The outburst flood resulting from failure of the Hyaloclastite Dam likely ranks within the top 10 floods documented in the United States and within the top 30 floods (>10^5 m^3 s^{-1}) recorded worldwide (Table 2; Fig. 5). This flood is definitely the largest known event in Grand Canyon and well illustrates the potential catastrophic consequences of the interaction of lava flows with a river within a deep bedrock canyon. Within our experience, this is the only study that quantitatively reconstructs the discharge of a flood resulting from a lava-dam failure and is the oldest flood with an estimated peak discharge, worldwide.

Acknowledgments

Peter Griffiths and Chris Magirl provided invaluable expertise and critical discussions. Kyle House, Jim O'Connor, Tom Hanks, Wayne Erskine, and an anonymous reviewer critically reviewed early drafts of the manuscript. The Geological Society of America, National Science Foundation, the U.S. Geological Survey, and the Grand Canyon Monitoring and Research Center provided funding or logistical support for this research.

References

Baker, V.R., Nummedal, D., 1978. The Channeled Scabland; A guide to the geomorphology of the Columbia Basin: Washington, DC, National Aeronautics and Space Administration, Planetary Geology Program Publication (186 pp).

Brunner, G.W., 2002. HEC-RAS River Analysis System User's Manual, Army Corps of Engineers. Hydrologic Engineering Center.

Bureau of Reclamation, 1990. Colorado river basin probable maximum floods: hoover and glen canyon dams. Department of the Interior, Washington, DC, U.S. (103 pp.)

Costa, J.E., O'Connor, J.E., 1995. Geomorphically effective floods. Natural and1 Anthropogenic Influences in Fluvial Geomorphology. Geophysical Monograph, vol. 89, pp. 45–56.

Dalrymple, G.B., Hamblin, W.K., 1998. K–Ar ages of Pleistocene lava dams in the Grand Canyon in Arizona. Proceedings of the National Academy of Sciences 95, 9,744–9,749.

Enzel, Y., Ely, L.L., House, P.K., Baker, V.R., Webb, R.H., 1993. Paleoflood evidence for a natural upper bound to flood magnitudes in the Colorado River basin. Water Resources Research 29, 2287–2297.

Erskine, W.D., Peacock, C.T., 2002. Late Holocene flood plain development following a cataclysmic flood. In: Dyer, F.J., Thoms, M.C., Olley, J.M. (Eds.), The Structure, Function, and Management Implications of Fluvial Sedimentary Systems: International Association of Hydrologic Sciences, vol. 276, pp. 177–184.

Fenton, C.R., Webb, R.H., Pearthree, P.A., Cerling, T.E., Poreda, R.J., 2001. Displacement rates on the Toroweap and Hurricane faults: Implications for Quaternary downcutting in Grand Canyon. Geology 29, 1035–1038.

Fenton, C.R., Webb, R.H., Cerling, T.E., Poreda, R.J., Nash, B.P., 2002. Cosmogenic ^{3}He ages and geochemical discrimination of lava-dam outburst-flood deposits in western Grand Canyon, Arizona. In: House, P.K., Webb, R.H., Baker, V.R., Levish, D.R. (Eds.), Ancient Floods, Modern Hazards, Principles and Applications of Paleoflood Hydrology. Water Science and

Application Series, vol. 4. American Geophysical Union, Washington, DC, pp. 191–215.

Fenton, C.R., Poreda, R.J., Nash, B.P., Webb, R.H., Cerling, T.E., 2004. Geochemical discrimination of five Pleistocene lava-dam outburst-flood deposits, Grand Canyon. Journal of Geology 112, 91–110.

Fread, D.L., Lewis, J.M., 1998. NWS HEC-RAS model: Silver Spring, Maryland, NOAA, National Weather Service, Hydrologic Research Laboratory (variable pages).

Garrett, J.M. and Gellenbeck, D.J., 1989. Basin characteristics and streamflow statistics in Arizona as of 1989. U.S. Geological Survey Water-Resources Investigational Report 91-4041.

Griffiths, P.G., Webb, R.H., Melis, T.S., 2004. Initiation and frequency of debris flows in Grand Canyon, Arizona. Journal of Geophysical Research 109, F04002 (doi:10.1029/2003JF000077, 14 pp.).

Hamblin, W.K., 1994a. Late Cenozoic lava dams in the western Grand Canyon. Geological Society of America Memoir 183 (139 pp.).

Hamblin, W.K., 1994b. Rates of erosion by the Colorado River in the Grand Canyon, Arizona. Proceedings of the 29th International Geology Congress, Part B, pp. 211–218.

Hanks, T.C., Webb, R.H., in press. Effects of tributary debris on the longitudinal profile of the Colorado River in Grand Canyon. Journal of Geophysical Research: Surface Processes.

Huscroft, C.A., Ward, B.C., Barendregt, R.W., Jackson Jr., L.E., Opdyke, N.D., 2004. Pleistocene volcanic damming of Yukon River and the maximum age of the Reid Glaciation, west-central Yukon. Canadian Journal of Earth Sciences 41, 151–164.

Jarrett, R.D., England Jr., J.F., 2002. Reliability of paleostage indicators for paleoflood studies. In: House, P.K., Webb, R.H., Baker, V.R., Levish, D.R. (Eds.), Ancient Floods, Modern Hazards, Principles and Applications of Paleoflood Hydrology. Water Science and Application Series, vol. 4. American Geophysical Union, Washington, DC, pp. 359–385.

Kaufmann, D., O'Brien, G., Mead, J.I., Bright, J., Umhoefer, P., 2002. Late Quaternary spring-fed deposits in the eastern Grand Canyon and their implications for deep lava-dammed lakes. Quaternary Research 58, 329–340.

Lucchitta, I., Curtis, G., Davis, M.E., Davis, S.W., Turrin, B., 2000. Cyclic aggradation and downcutting, fluvial response to volcanic activity, and calibration of soil-carbonate stages in the western Grand Canyon, Arizona. Quaternary Research 53, 23–33.

McIntosh, W.C., Peters, L., Karlstrom, K.E., Pederson, J.L., 2002. New ^{40}Ar–^{39}Ar dates on basalts in Grand Canyon: constraints on rates of Quaternary river incision and slip on the Toroweap fault and implications for lava dams. Geological Society of America Abstracts with Program, Rocky Mountain Section 34 (4), 61.

O'Connor, J.E., 1993. Hydrology, hydraulics, and geomorphology of the Bonneville flood. Geological Society of America, Special Paper 274, 83 pp.

O'Connor, J.E., Ely, L.L., Wohl, E.E., Stevens, L.E., Melis, T.S., Kale, V.S., Baker, V.R., 1994. A 4500-year record of large floods on the Colorado River in the Grand Canyon, Arizona. Journal of Geology 102, 1–9.

O'Connor, J.E., Grant, G.E., Costa, J.E., 2002. The geology and geography of floods. In: House, P.K., Webb, R.H., Baker, V.R., Levish, D.R. (Eds.), Ancient Floods, Modern Hazards, Principles and Applications of Paleoflood Hydrology. Water Science and Application Series, vol. 4. American Geophysical Union, Washington, DC, pp. 359–385.

Pederson, J., Karlstrom, K., Sharp, W., McIntosh, W., 2002. Differential incision of the Grand Canyon related to Quaternary faulting—Constraints from U-series and Ar/Ar dating. Geology 739–742.

Stockton, C.W., Jacoby Jr., J.C., 1976. Long-term surface-water supply and streamflow trends in the upper Colorado River basin. Lake Powell Research Project Bulletin 18 (70 pp.).

Teller, J.T., Thorleifson, L.H., 1987. The Lake Agassiz-Lake Superior connection. In: Mayer, L., Nash, D. (Eds.), Catastrophic Flooding. Allen and Unwin, Boston, Massachusetts, pp. 121–138.

Topping, D.J., Schmidt, J.C., Vierra, L.E., Jr., 2003. Computation and analysis of the instantaneous-discharge record for the Colorado River at Lees Ferry, Arizona; May 8, 1921, through September 30, 2000. U.S. Geological Survey Professional Paper 1677 (118 pp).

Trabant, D.C., March, R.S., Thomas, D.S., 2003. Hubbard Glacier, Alaska: Growing and advancing in spite of global climate change and the 1986 and 2002 Russell Lake outburst floods. U.S. Geological Survey Fact Sheet 001–03 (4 pp).

United States Geological Survey, 1924. Plan And profile of Colorado River from Lees Ferry Ariz., to Black Canyon, Ariz.- Nev. and Virgin River, Nev. U.S. Geological Survey Map report.

Walder, J.S., Driedger, C.L., 1994. Geomorphic change caused by outburst floods and debris flows at Mount Rainier, Washington, with emphasis on Tahoma Creek Valley: U.S. Geological Survey Water-Resources Investigations Report. 93-4093 (93 pp).

Walder, J.S., O'Connor, J.E., 1997. Methods for predicting peak discharge of floods caused by failure of natural and constructed earthen dams. Water Resources Research 33, 2348–2377.

Walker, N.D., Lawrence Jr., J.R., Fargion, G.S., Biggs, D.C., 1994. The great flood of Summer 1993: Mississippi River discharge studied. Earth in Space 7, 11–14.21.

Waythomas, C.R., Walder, J.S., McGimsey, R.G., Neal, C.A., 1996. A catastrophic flood caused by drainage of a caldera lake at Aniakchak volcano, Alaska, and implications for volcanic-hazards assessment. Geological Society of America Bulletin 108, 861–871.

Webb, R.H., Blainey, J.B., Hyndman, D.W., 2002. Paleoflood hydrology of the Paria River, southern Utah and northern Arizona, USA. In: House, P.K., Webb, R.H., Baker, V.R., Levish, D.R. (Eds.), Ancient Floods, Modern Hazards, Principles and Applications of Paleoflood Hydrology. Water Science and Application Series, vol. 5. American Geophysical Union, Washington, DC, pp. 295–310.

Wenrich, K.J., Billingsley, G.H., Blackerby, B.A., 1995. Spatial migration and compositional changes of Miocene-Quaternary magmatism in the western Grand Canyon. Journal of Geophysical Research 100, 10417–10440.